Electronic Supplementary Material (ESI) for Physical Chemistry Chemical Physics.
This journal is © the Owner Societies 2018

# Interface engineering and solid-state organization for triindole-based p-type Organic Thin-Film Transistors

Marta Reig,[a] Gintautas Bagdziunas,[b,c] Arunas Ramanavicius,[b,c]

Joaquim Puigdollers[d] and Dolores Velasco*[a]

[a] Grup de Materials Orgànics, Institut de Nanociència i Nanotecnologia (IN$^2$UB), Departament de Química Inorgànica i Orgànica, Secció de Química Orgànica, Universitat de Barcelona, Martí i Franquès 1, E-08028, Barcelona, Spain

[b] Department of Material Science and Electrical Engineering, State Research Institute Centre for Physical Sciences and Technology, Sauletekio Av. 3, LT-10257, Vilnius, Lithuania

[c] Department of Physical Chemistry, Vilnius University, Faculty of Chemistry and Geosciences, Naugarduko str. 24, Vilnius, Lithuania

[d] Dept. Enginyeria Electrònica, Universitat Politècnica de Catalunya, C/ Jordi Girona 1–3, E-08034, Barcelona, Spain

** Corresponding author: D. Velasco. E-mail: dvelasco@ub.edu*

## Contents

**Scheme S1** Synthesis of triindole derivatives **1**–**3** ..... S1

**Figure S1** UV-Vis absorption spectra of **1**–**3** ..... S2
**Figure S2** Cyclic voltammograms of **1**–**3** ..... S2
**Figure S3** Crystal structures of **2** and **3** ..... S3
**Figure S4–S6** OTFT characteristics of **1**–**3** ..... S3
**Figure S7** Intermolecular interactions in **1** estimated by DFT calculations ..... S5
**Figure S8** XRD patterns of thin films of **2** ..... S5

**Table S1** Crystallographic data of **3** ..... S6
**Table S2** Theoretical calculation data of the hole and electron mobilities of **1**–**3** ..... S7
**Table S3** Computed dielectric constants, molecular volumes and static isotropic polarizabilities ..... S7

## SCHEMES

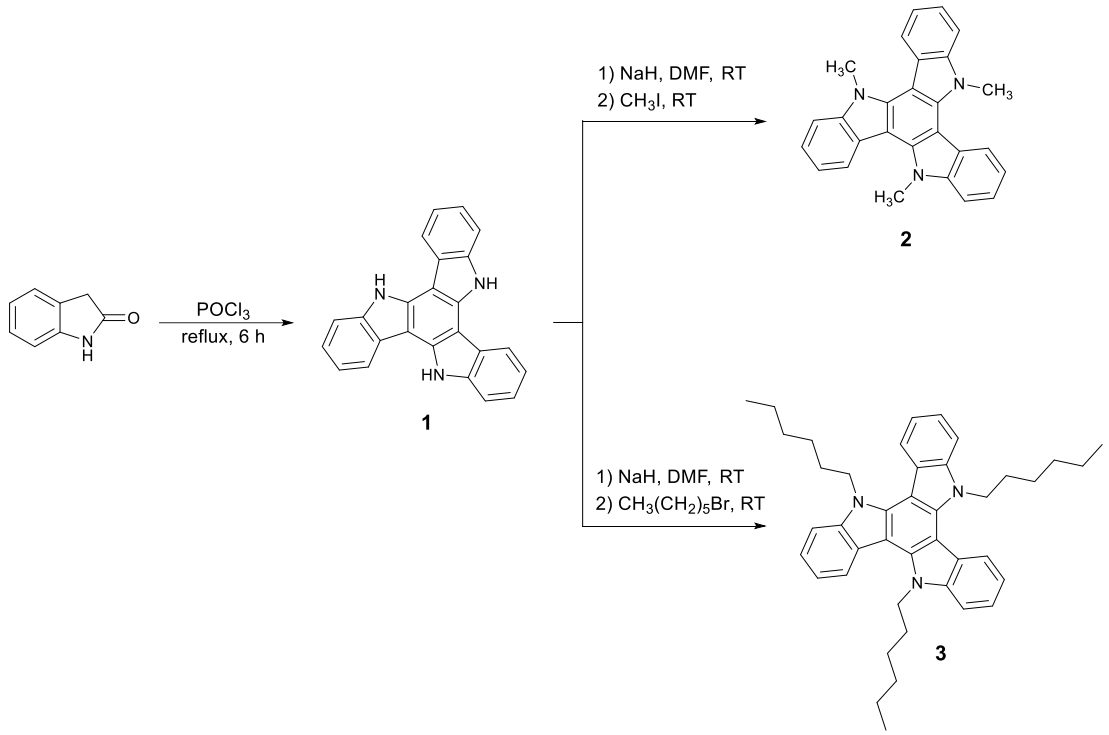


**Scheme S1.** Synthesis of triindole derivatives **1**–**3**.

## FIGURES

The UV-vis absorption spectra of triindole derivatives **1**–**3** in 10 µM dichloromethane solutions display the absorption maximum in the UV zone in the range of 306–318 nm (Table 1 and Figure S1). The alkylation of the nitrogen atoms of triindole derivatives **2** and **3** implies a red shift of 11–12 nm of the wavelength of maximum absorption, in comparison to the non-alkylated derivative **1**.

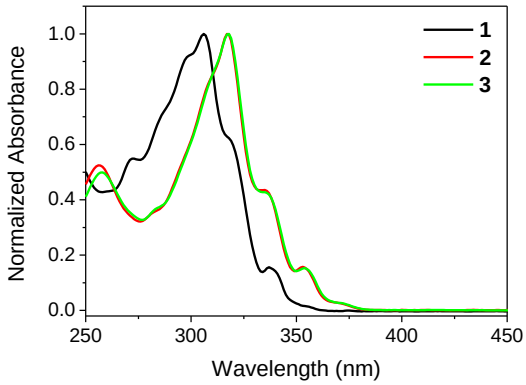


**Figure S1.** UV-Vis absorption spectra of **1**–**3** recorded in 10 µM dichloromethane solutions at room temperature.

Compound **1** showed irreversible oxidation processes by cyclic voltammetry, whereas *N*-alkylated triindole derivatives **2** and **3** showed two oxidation processes, being the first one quasi-reversible (Figure S2). No reduction processes were observed for any of them.

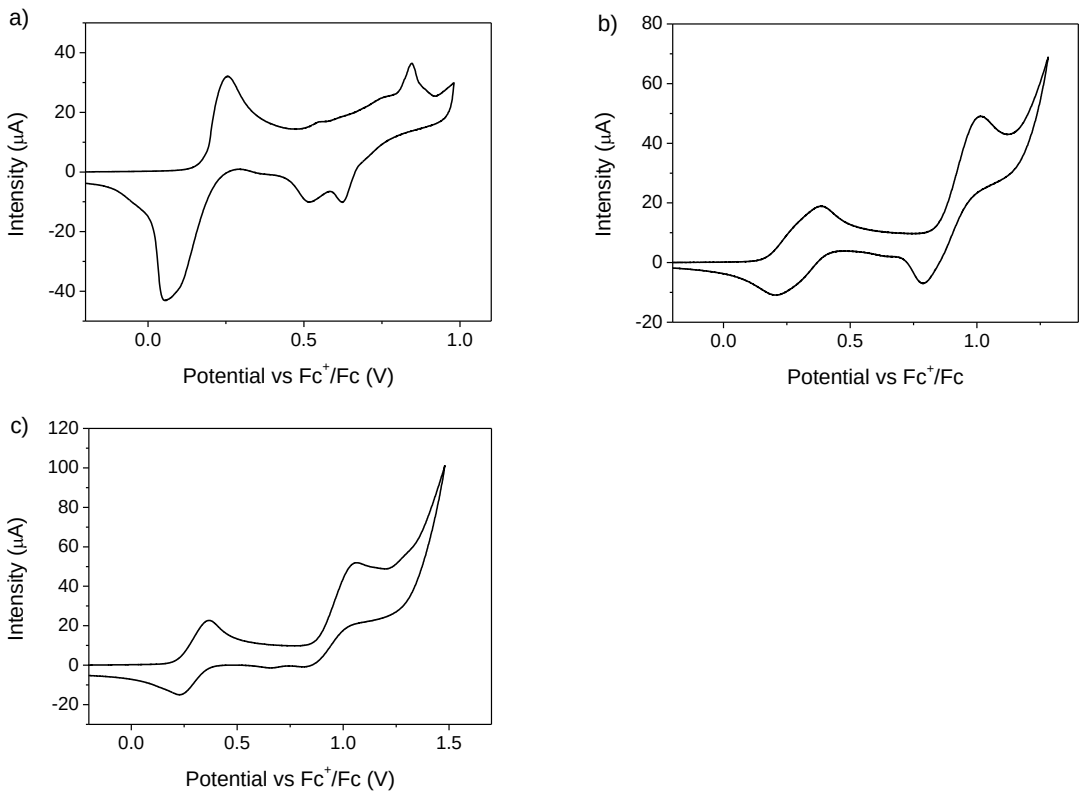


**Figure S2.** Cyclic voltammograms of a) **1**, b) **2** and c) **3** recorded at a scan rate of 100 mV $s^{-1}$ in 1 mM dichloromethane solutions (1 mM).

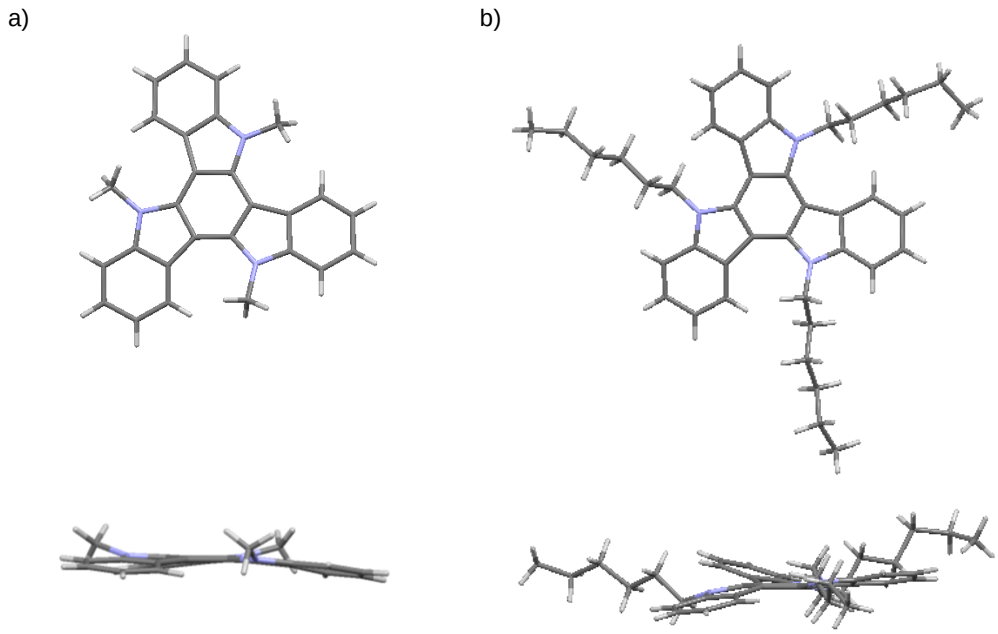


**Figure S3.** Crystal structures of a) **2**[1] and b) **3**.

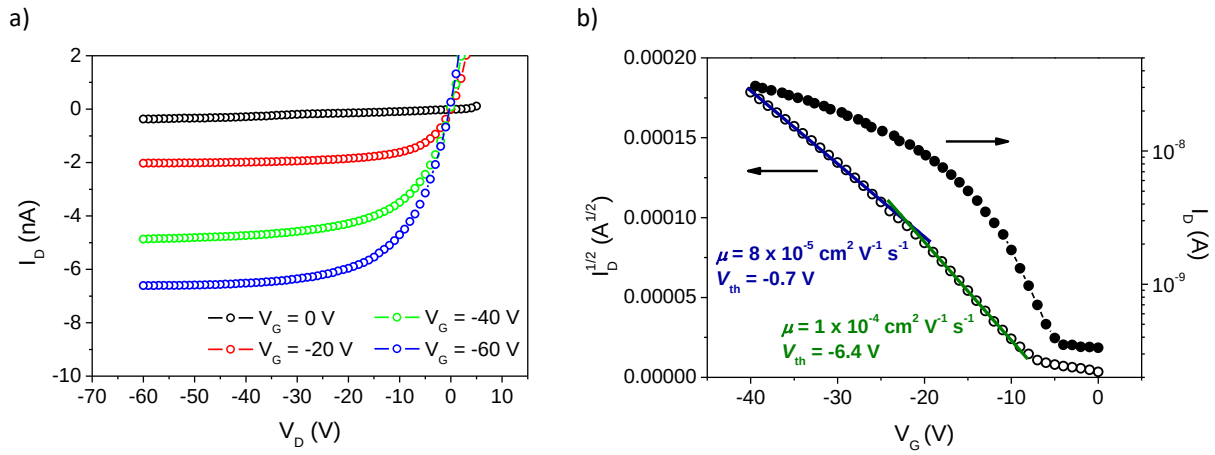


**Figure S4.** OTFT characteristics of a device fabricated with **1** as the semiconductor layer and with OTS-treated c-Si/$SiO_2$ substrate. a) Output characteristics at different gate voltages ($V_G$). b) Transfer ($V_D$ = –40 V) and saturation characteristics.

[1] E. M. García-Frutos, E. Gutierrez-Puebla, M. A. Monge, R. Ramírez, P. de Andrés, A. de Andrés, R. Ramírez and B. Gómez-Lor, *Org. Electron.* 2009, **10**, 643–652.

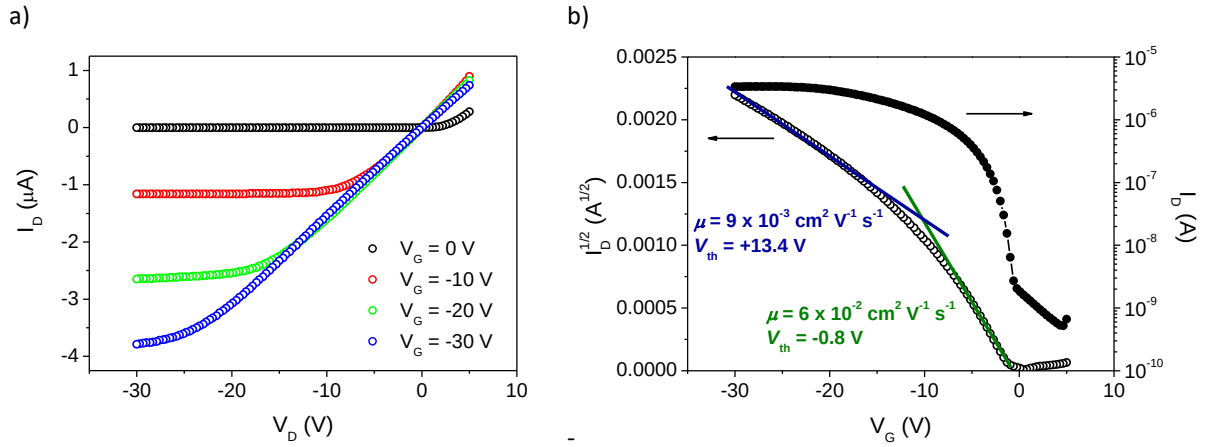


**Figure S5.** OTFT characteristics of a device fabricated with **2** as the semiconductor layer and with OTS-treated c-Si/$SiO_2$ substrate. a) Output characteristics at different gate voltages ($V_G$). b) Transfer ($V_D$ = –20 V) and saturation characteristics.

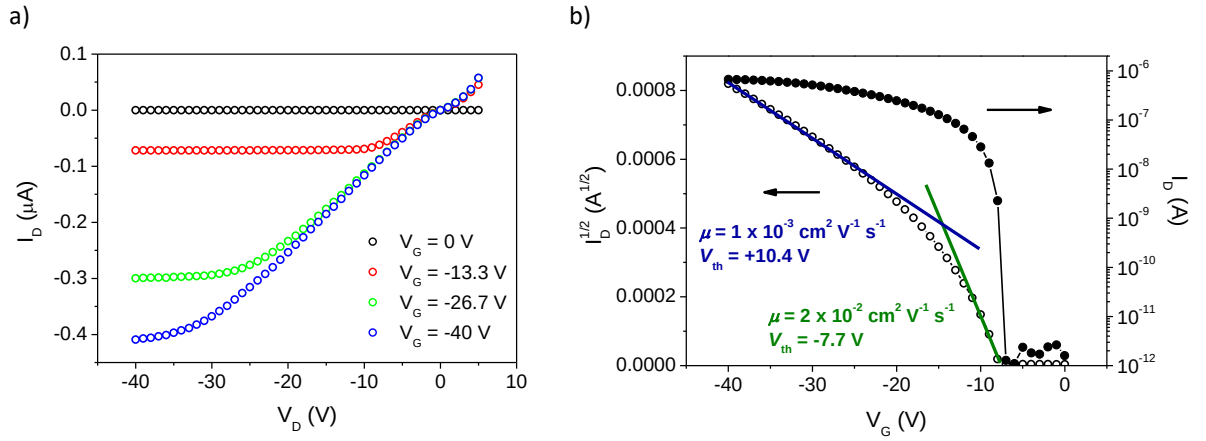


**Figure S6.** OTFT characteristics of a device fabricated with **3** as the semiconductor layer and with OTS-treated c-Si/$SiO_2$ substrate. a) Output characteristics at different gate voltages ($V_G$). b) Transfer ($V_D$ = –40 V) and saturation characteristics.

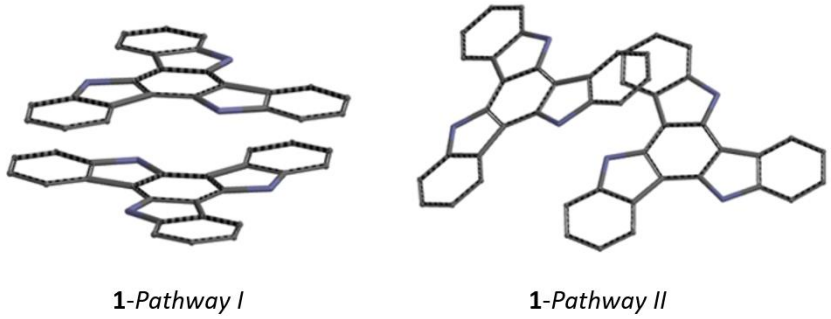


**Figure S7.** Intermolecular interactions between neighbouring molecules in compound **1** estimated by DFT. The hydrogen atoms were omitted for clarity.

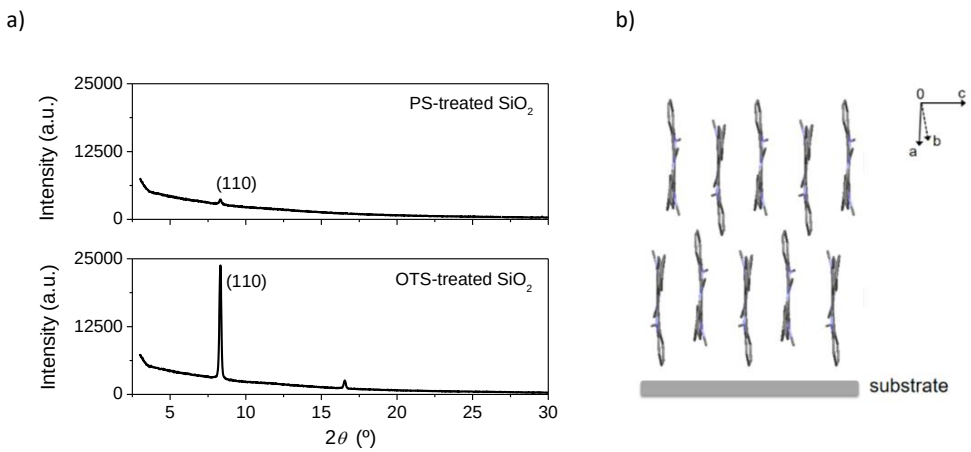


**Figure S8.** XRD patterns of vacuum-deposited **2** films on PS and OTS-treated c-Si/$SiO_2$ surfaces. b) Molecular packing in the thin film with the (110) plane situated perpendicular to the paper. The hydrogen atoms were omitted for clarity.

## TABLES

**Table S1.** Crystal data and structure refinement for *N*-trihexyltriindole (**3**).

| | | |
|---|---|---|
| Identification code | N-Trihexyltriindole | |
| Empirical formula | C42 H51 N3 | |
| Formula weight | 597.85 | |
| Temperature | 100(2) K | |
| Wavelength | 0.71073 Å | |
| Crystal system | Triclinic | |
| Space group | P -1 | |
| Unit cell dimensions | a = 8.411(3) Å | $\alpha$= 86.900(16)°. |
| | b = 15.202(5) Å | $\beta$= 89.438(15)°. |
| | c = 26.348(9) Å | $\gamma$ = 84.427(17)°. |
| Volume | 3348.2(19) $Å^3$ | |
| Z | 4 | |
| Density (calculated) | 1.186 $Mg/m^3$ | |
| Absorption coefficient | 0.069 $mm^{-1}$ | |
| F(000) | 1296 | |
| Crystal size | 0.382 x 0.108 x 0.034 $mm^3$ | |
| Theta range for data collection | 2.106 to 26.893°. | |
| Index ranges | -10<=h<=10, -19<=k<=19, -33<=l<=33 | |
| Reflections collected | 61914 | |
| Independent reflections | 13846 [R(int) = 0.0870] | |
| Completeness to theta = 25.242° | 99.9 % | |
| Absorption correction | Semi-empirical from equivalents | |
| Max. and min. transmission | 0.7454 and 0.5392 | |
| Refinement method | Full-matrix least-squares on $F^2$ | |
| Data / restraints / parameters | 13846 / 2 / 799 | |
| Goodness-of-fit on $F^2$ | 0.866 | |
| Final R indices [I>2sigma(I)] | R1 = 0.0795, wR2 = 0.1683 | |
| R indices (all data) | R1 = 0.2746, wR2 = 0.2293 | |
| Extinction coefficient | n/a | |
| Largest diff. peak and hole | 0.740 and -0.540 e.$Å^{-3}$ | |

**Table S2.** Theoretical calculation data of hole and electron mobilities of **1**–**3**.

| Compound | Pathway | $d$ [b] (Å) | $H_h$ [c] (meV) | $H_e$ [c] (meV) | $k_h \times 10^{12}$ [d] ($s^{-1}$) | $k_e \times 10^{12}$ [d] ($s^{-1}$) | $-E_i$ [e] (kJ $mol^{-1}$) |
|---|---|---|---|---|---|---|---|
| **1** [a] | I | 3.7 | 0.20 | 0.15 | 0.00020 | 0.00026 | 113.2 |
| **1** [a] | II | 6.6 | 87.1 | 83.1 | 0.026 | 9.0 | 90.1 |
| **2** | I | 3.9 | 51.3 | 41.9 | 4.5 | 3.0 | 137.1 |
| **2** | II | 3.8 | 122 | 79.9 | 29 | 12 | 151.0 |
| **2** | III | 12.6 | 8.9 | 15.6 | ~0 | ~0 | 8.48 |
| **3** | I | 4.4 | 66.1 | 41.2 | 6.0 | 2.5 | 158.6 |
| **3** | II | 10.2 | 10.5 | 17.0 | ~0 | ~0 | 46.9 |
| **3** | III | 13.2 | 29.3 | 32.5 | ~0 | ~0 | 82.6 |

[a] The structures of dimers were optimized using wB97X-D/6-31G(d,p) method.
[b] Distance between the neighbouring moieties in dimer *i*.
[c] Coupling integrals for holes ($H_h$) and for electrons ($H_e$).
[d] Electron transfer rate constant for holes ($k_h$) and for electrons ($k_e$).
[e] Interaction energy between neighbouring molecules.

**Table S3.** Computed static isotropic polarizabilities, molecular volumes (with Van der Waals radius of 1 Å) and dielectric constants.

| Compound | α (Å$^3$) | V (Å$^3$) | ε |
|---|---|---|---|
| **1** | 68.9 | 653 | 3.4 |
| **2** | 73.5 | 737 | 3.2 |
| **3** | 95.8 | 1131 | 2.6 |